Journal of Saudi Chemical Society (2011) **15**, 105–112

King Saud University

Journal of Saudi Chemical Society

www.ksu.edu.sa
www.sciencedirect.com

ORIGINAL ARTICLE

Removal of nickel (II) from aqueous solutions by using nano-crystalline calcium hydroxyapatite

I. Mobasherpour [a], E. Salahi [a,*], M. Pazouki [b]

[a] *Ceramics Department, Materials and Energy Research Center, P.O. Box 31787-316, Karaj, Iran*
[b] *Energy Department, Materials and Energy Research Center, P.O. Box 31787-316, Karaj, Iran*

Received 1 May 2010; accepted 12 June 2010
Available online 18 June 2010

KEYWORDS

Adsorption;
Nano-crystalline hydroxyapatite;
Heavy metal;
Ni^{2+} ion;
Isotherms

Abstract The potential of the synthesized nano-hydroxyapatite to remove Ni^{2+} from aqueous solutions was investigated in batch reactor under different experimental conditions. The study also investigates the effects of process parameters such as initial concentration of Ni^{2+} ion, temperature, and adsorbent mass. Various thermodynamic parameters, such as ΔG°, ΔH° and ΔS° have been calculated. The thermodynamics of Ni^{2+} ion onto nano-HAp system indicates spontaneous and endothermic nature of the process. Nickel uptake was quantitatively evaluated using the Langmuir, Freundlich and Dubinin–Kaganer–Radushkevich model. The adsorption data follow the adsorption equilibrium was described well by the Langmuir isotherm model with maximum adsorption capacity of 46.17 mg/g of Ni^{2+} ions on nano-HAp.

1. Introduction

Because of heavy metals toxicity and non-biodegradable nature, the introduction of heavy metals in water is becoming a serious environmental and public health concern. A number of technologies have been developed to remove toxic heavy metals from wastewater.

Furthermore, automotive, electronics, metal finishing and oil sands industries form a large economic sector in Iran. These industries generate a large quantity of wastewater containing heavy metals such as Pb^{2+}, Cd^{2+}, Zn^{2+}, Ni^{2+} and others. Typically, the wastewater from the metal finishing industry (e-coating process) contains 20 ppm each of Zn^{2+} and Ni^{2+}. On the other hand, the maximum allowable discharge concentration of Zn^{2+} and Ni^{2+} is 2 ppm (Doan et al., 2006).

Various methods have been used to remove heavy metals from wastewater, including: reduction and precipitation (Esalah et al., 2000), coagulation and flotation (Zouboulis et al., 1997), adsorption (Toles and Marshall, 2002; Ravindran et al., 1999), ion exchange, membrane technologies and electrolysis (Canet et al., 2002). Generally, they are expensive or ineffective, especially when the metal concentration is higher than 100 ppm (Miretzky et al., 2006; Schiewer and Volesky, 1995).

* Corresponding author. Tel.: +98 261 6204131.
E-mail addresses: e-salahi@merc.ac.ir, kesalahi@yahoo.com (E. Salahi).

1319-6103

Peer review under responsibility of King Saud University.
doi:10.1016/j.jscs.2010.06.003

Production and hosting by Elsevier

Hydroxyapatite is an ideal material for long-term containment of contaminants because of its high sorption capacity for actinides and heavy metals, low water solubility, high stability under reducing and oxidizing conditions, availability, and low cost (Krestou et al., 2004). It was conducted in stabilization of a wide variety of metals (e.g., Cr, Co, Cu, Cd, Zn, Ni, Pu, Pb, As, Sb, U, and V) by many investigators (Czerniczyniec et al., 2003; Vega et al., 1999; Reichert and Binner, 1996; Leyva et al., 2001; Fuller et al., 2002; McGrellis et al., 2001). They reported the sorption to take place through ionic exchange reaction, surface complexation with phosphate, calcium and hydroxyl groups and/or co-precipitation of new partially soluble phases.

Calcium hydroxyapatite (CaHAp), $Ca_{10}(PO_4)_6(OH)_2$, is used for the removal of heavy metals from contaminated soils, wastewater and fly ashes (Chen et al., 1997; Laperche et al., 1996; Ma et al., 1993, 1994; Mavropoulos et al., 2002; Nzihou and Sharrock, 2002; Takeuchi and Arai, 1990). Calcium hydroxyapatite (CaHAp) is a principal component of animal hard tissues and has been of interest in industry and medical fields. Its synthetic particles find many applications in bioceramics, chromatographic adsorbents to separate protein and enzyme, catalysts for dehydration and dehydrogenation of alcohols, methane oxidation, and powders for artificial teeth and bones paste germicides (Elliott, 1994). These properties relate to various surface characteristics of HAp, e.g., surface functional groups, acidity and basicity, surface charge, hydrophilicity, and porosity. It has been found that HAp surface possesses 2.6 groups nm^{-2} of P—OH groups acting as sorption sites (Tanaka et al., 2005). The sorption properties of HAp are of great importance for both environmental processes and industrial purposes.

The objective of this study was to investigate the possible use of nano-crystalline hydroxyapatite as an alternative adsorbent material for removal of Ni^{2+} ions from aqueous solutions. The Langmuir, Freundlich and D–R models were used to fit the equilibrium isotherm. The dynamic behavior of the adsorption was investigated on the effect of initial metal ion concentration, temperature, and adsorbent mass of solution. The thermodynamic parameters were also evaluated from the adsorption measurements.

2. Material and methods

2.1. Sorption study

All sorption experiments were carried without any pre-equilibrium processes were imposed during the performance of any experiments. In order to determine the sorption capacity of nano-HAp for Ni^{2+} cations, as well as the influence of the initial concentration of Ni^{2+} ion, adsorbent dosage and temperature, sorption experiments were performed by batch equilibration technique.

Aqueous solutions containing Ni^{2+} ions of concentration (30, 40, 60 and 80 mg/L) were prepared from Ni^{2+} sulfate ($NiSO_4{\cdot}7H_2O$, Merck No. 6725). A 0.4 g of nano-HAp were introduced in a stirred tank reactor containing 500 ml of the prepared solution. The stirring speed of the agitator was 300 rpm. The temperature of the suspension was maintained at 20 ± 1 °C. the initial pH of the solution was adjusted to the value 6.6 by adding NH_3 and HCl. Samples were taken after mixing the adsorbent and Ni^{2+} ion bearing solution at pre determined time intervals (5, 10, 20, 30, 60 and 120 min) for the measurement of residual metal ion concentration in the solution and to ensure equilibrium was reached. After any specified time the sorbents were separated from the solution by centrifuge and filtration through the filter paper (Whatman grade 6). The exact concentration of metal ions was determined by AAS (GBC 932 Plus atomic absorption spectrophotometer). All experiments were carried out twice.

2.2. Preparation of nano-crystalline hydroxyapatite sorbents

All chemicals used in this work were of analytical grade and the aqueous solutions were prepared using double distilled water. Nano-crystalline hydroxyapatite compounds were prepared by a solution–precipitation method (Mobasherpour et al., 2007) using $(NH_4)_2HPO_4$ (Merck No. 1205) and $Ca(NO_3)_2{\cdot}4H_2O$ (Analar No. 10305) as starting materials and ammonia solution as agents for pH adjustment. A suspension of $Ca(NO_3)_2{\cdot}4H_2O$ was vigorously stirred and its temperature was maintained at 25 °C. A solution of $(NH_4)_2HPO_4$ was slowly added dropwise to the $Ca(NO_3)_2{\cdot}4H_2O$ solution. In all experiments the pH of $Ca(NO_3)_2{\cdot}4H_2O$ solution by adding ammonia solution was 11. The precipitate HAP was removed from solution by the centrifuge method at a rotation speed of 3000 rpm. The resulting powder was dried at 100 °C. The particles thus synthesized were characterized by the following methods. Transmission electron microscopy (TEM) was used to characterize the synthesized particles of HAp. For this purpose, particles were deposited onto Cu grids, which support a "holey" carbon film. The particles were deposited onto the support grids by deposition from a dilute suspension in acetone or ethanol. The crystalline shapes and sizes were characterized by diffraction (amplitude) contrast and, for crystalline materials, by high resolution (phase contrast) imaging. The specific surface area was determined from N_2 adsorption isotherm by the BET method using a Micromeritics surface area analyzer model ASAP 2010. The crystal phase was identified by powder X-ray diffraction (XRD) using Siemens (30 kV and 25 mA) X-ray diffractometer with Cu Kα radiation ($\lambda = 1.5404$ Å) and XPERT software.

3. Results and discussion

3.1. Characteristics of adsorbent

TEM micrograph of the HAp powders after drying is seen in Fig. 1(a). The microstructure of the HAp crystalline after drying is observed be almost like needle shape, with size in the range 20–30 nm. The crystal structure analysis of HAp particles was performed, using X-ray diffraction, and the obtained diffractograms are represented in Fig. 1(b). The produced reflection patterns match the ICDD standards (JCPDS) for HAp. The patterns show only the peaks characteristic to the synthesized HAp with no obvious evidences on the presence of other additional phases. The broad patterns around (2 1 1) and (0 0 2) indicate that the crystallites are very tiny in nature with much atomic oscillations. The analysis of the HAp sample has confirmed a low-crystalline product, with the specific surface area 94.9 m^2/g.

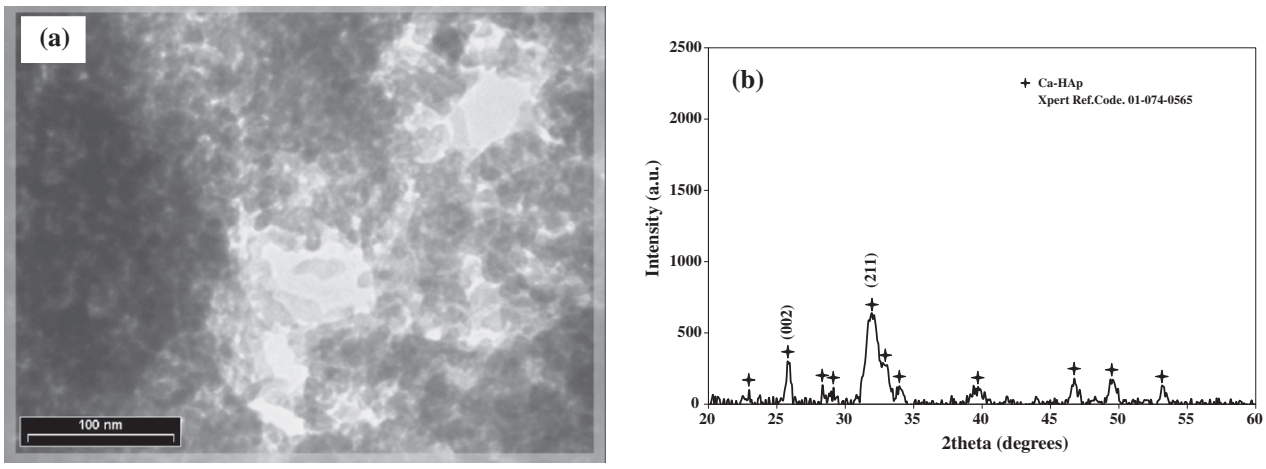

Figure 1 TEM micrograph (a) and XRD pattern (b) of the calcium nano-crystalline hydroxyapatite after drying at 100 °C.

3.2. Effect of initial Ni^{2+} concentration and adsorbent dosage

The sorption of Ni^{2+} ions was carried out at different initial Ni^{2+} ion concentrations ranging from 40 to 80 mg/L, at pH 6.6, at 300 rpm with 120 min of contact time using nano-HAp. A rapid kinetic reaction of Ni removal by sorbent occurred within the first 5 min (Fig. 2(a)). The aqueous Ni concentration at 5 min decreased to 18, 34 and 51 mg/L by nano-HAp for 40, 60 and 80 mg/L initial concentration, respectively.

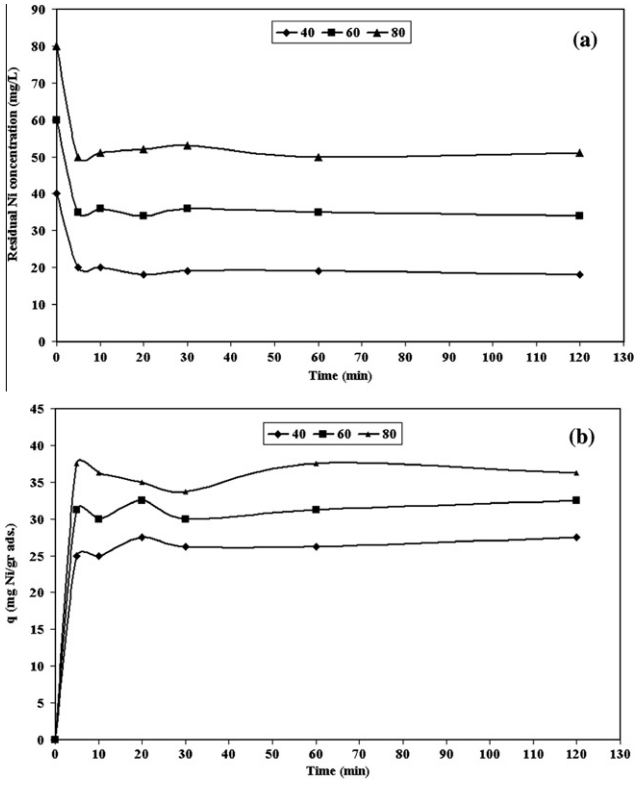

Figure 2 Time dependent concentration (a) and effect of initial concentration of nickel (b) on removal of aqueous Ni^{2+} by nano-hydroxyapatite sorbents (pH 6.6, adsorbent dosage = 0.8 g/L, 300 rpm agitating rate).

Uptake of the Ni^{2+} also increased with increasing the initial metal concentration tending to saturation at higher metal concentrations. As shown in Fig. 2(b), when the initial Ni^{2+} concentration increased from 40 to 80 mg/L, the uptake capacity of nano-HAp increased from 27.50 to 36.25 mg/g. A higher initial concentration provides an important driving force to overcome all mass transfer resistances of the pollutant between the aqueous and solid phases, thus increases the uptake (Aksu and Tezer, 2005).

The effect of nano-HAp dosage is presented in Fig. 3. It is evident that adsorption increases with the increase in the mass of sorbent and the uptake capacity of Ni^{2+} decreased from 36.25 mg/g (36.25% removal) to 19.37 mg/g (38.75% removal) with the increasing nano-HAp concentration from 0.8 to 1.6 g/L. This is because at the higher dosage of sorbent due to increased surface area, more adsorption sites are available causing higher removal of Ni^{2+}.

3.3. Effect of temperature

To study the effect of this parameter on the uptake of Ni^{2+} ions by nano-HAp, we selected the following temperature: 20, 50 and 70 °C. Fig. 4 illustrates the relationship between temperature and the amount of Ni^{2+} ions adsorbed onto

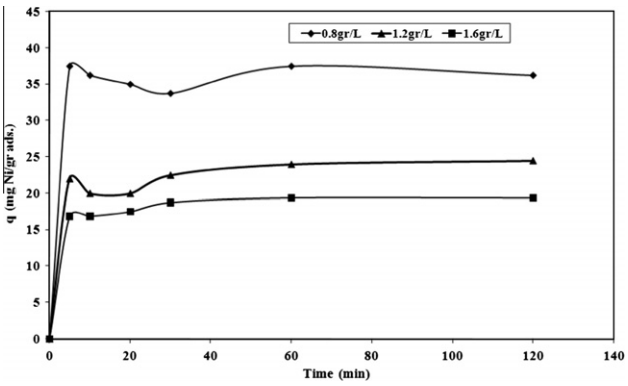

Figure 3 Effect of adsorbent dosage on removal of Ni^{2+} by nano-hydroxyapatite (pH 6.6, initial metal concentration = 80 mg/L, 300 rpm agitating rate).

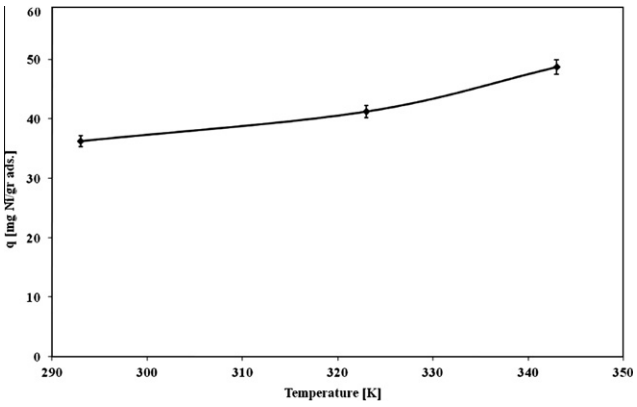

Figure 4 The uptake capacity of Ni^{2+} ions at different temperature (pH 6.6, initial metal concentration = 80 mg/L, adsorbent dosage = 0.8 g/L, 300 rpm agitating rate).

nano-HAp at equilibrium time (120 min). As seen in Fig. 4, the adsorption of Ni^{2+} on nano-HAp increased from 36.25 to 48.75 mg/g when temperature was increased from 20 to 70 °C at an initial concentration of 80 mg/L. The increase in the equilibrium sorption of Ni^{2+} with temperature indicates that Ni^{2+} ions removal by adsorption on nano-HAp favors a high temperature. This may be a result of increase in the mobility of the Ni^{2+} ion with temperature. An increasing number of molecules may also acquire sufficient energy to undergo an interaction with active sites at the surface. Furthermore, increasing temperature may produce a swelling effect within the internal structure of the nano-HAp enabling metal ions to penetrate further (Dŏgan and Alkan, 2003).

3.4. Determination of thermodynamic parameters

Thermodynamic parameters such as free energy change (ΔG°), enthalpy change (ΔH°), and entropy change (ΔS°) can be estimated using equilibrium constants changing with temperature. The free energy change of the sorption reaction is given by the following equation:

$$\Delta G^\circ = -RT \ln K_d \tag{1}$$

where ΔG° is standard free energy change (J); R is the universal gas constant, 8.314 J/mol K and T is the absolute temperature (K).

The distribution ratio (K_d) was calculated using the below equation:

$$K_d = \frac{\text{amount of metal in adsorbent}}{\text{amount of metal in solution}} \times \frac{V}{m} \tag{2}$$

where V is the volume of the solution (ml) and m is the weight of the adsorbent (g).

$$\Delta G^\circ = \Delta H^\circ - T\Delta S^\circ \tag{3}$$

The distribution ratio (K_d) values increased with temperature, indicating the endothermic nature of adsorption. A plot of Gibbs free energy changes, ΔG°, versus temperature, T (K); was found to be linear. The values of ΔH° and ΔS° were determined from the slope and intercept of the plots. The thermodynamic parameters Gibbs free energy change, ΔG°, are shown in Table 1. The enthalpy change, ΔH°, and the entropy change, ΔS°, for the sorption processes are calculated to be

Table 1 Thermodynamic parameters for the adsorption of Ni^{2+} onto nano-hydroxyapatite.

T (K)	K_d	ΔG° (J/mol)	ΔH° (J/mol)	ΔS° (J/mol K)
293	710.79	−15995.70		
323	877.66	−18199.80	8438.60	83.11
343	1189.03	−20192.60		

8438.60 J/mol and 83.11 J/mol K, respectively. The negative values of ΔG° at various temperatures indicate the spontaneous nature of the adsorption process. The positive value of ΔS° indicates that there is an increase in the randomness in the system solid/solution interface during the adsorption process. In addition, the positive value of ΔH° indicates that the adsorption is endothermic. The positive value of ΔS° reflects the affinity of the nano-HAp for Ni^{2+} ions and suggests some structural changes in nickel and nano-HAp (Ho, 2003).

3.5. Adsorption isotherms

Analysis of the equilibrium data is important to develop an equation which accurately represents the results and which could be used for design purposes (Aksu, 2002). Several isotherm equations have been used for the equilibrium modeling of adsorption systems.

The sorption data have been subjected to different sorption isotherms, namely, Langmuir, Freundlich, and Dubinin–Kaganer–Radushkevich.

The equilibrium data for metal cations over the concentration range from 30 to 80 mg/L at 20 °C have been correlated with the Langmuir isotherm (Langmuir, 1918):

$$\frac{C_e}{q_e} = \frac{1}{Q_0 K} + \frac{C_e}{Q_0} \tag{4}$$

where C_e is the equilibrium concentration of metal in solution (mg/L), q_e is the amount absorbed at equilibrium onto nano-HAp (mg/g), Q_0 and K are Langmuir constants related to sorption capacity and sorption energy, respectively. Maximum sorption capacity (Q_0) represents monolayer coverage of sorbent with sorbate and K represents enthalpy of sorption and should vary with temperature. A linear plot is obtained when C_e/q_e is plotted against C_e over the entire concentration range of metal ions investigated.

The linearized Langmuir adsorption isotherms of Ni^{2+} ions are given in Fig. 5(a). An adsorption isotherm characterized by certain constants which values express the surface properties and affinity of the sorbent and can also be used to find the sorption capacity of sorbent.

The Freundlich sorption isotherm, one of the most widely used mathematical descriptions, usually fits the experimental data over a wide range of concentrations. This isotherm gives an expression encompassing the surface heterogeneity and the exponential distribution of active sites and their energies. The Freundlich adsorption isotherms were also applied to the removal of Ni^{2+} on nano-HAp (Fig. 5(b)):

$$\ln q_e = \ln k_f + \frac{1}{n} \ln C_e \tag{5}$$

where q_e is the amount of metal ion sorbed at equilibrium per gram of adsorbent (mg/g), C_e the equilibrium concentration of metal ion in the solution (mg/L), k_f, and n the Freundlich

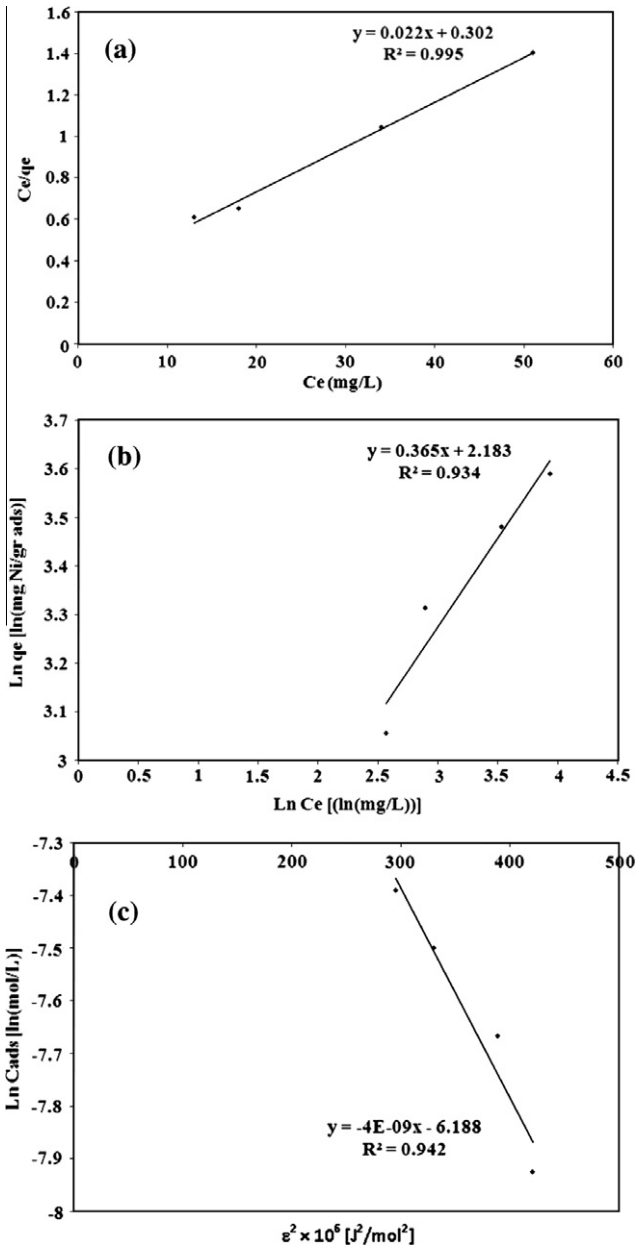

Figure 5 Linear fits of experimental data obtained using Langmuir (a), Freundlich (b) and D–R (c) sorption isotherms for the adsorption of Ni^{2+} onto nano-hydroxyapatite (pH 6.6, initial metal concentration = 30, 40, 60 and 80 mg/L, adsorbent dosage = 0.8 g/L, 300 rpm agitating rate).

model constants (Malkoc and Nuhŏglu, 2003; Kadirvelu et al., 2001). Freundlich parameters, k_f and n, were determined by plotting ln q_e versus ln C_e. The numerical value of $1/n < 1$ indicates that adsorption capacity is only slightly suppressed at lower equilibrium concentrations. This isotherm does not predict any saturation of the sorbent by the sorbate; thus infinite surface coverage is predicted mathematically, indicating multilayer adsorption on the surface (Hasany et al., 2002).

The Dubinin–Kaganer–Radushkevich (D–R) has been used to describe the sorption of metal ions on clays. The D–R equation has the form:

$$\ln C_{ads} = \ln X_m - \beta\varepsilon^2 \quad (6)$$

where C_{ads} is the number of metal ions adsorbed per unit weight of adsorbent (mol/g), X_m (mol/g) is the maximum sorption capacity, β (mol^2/J^2) is the activity coefficient related to mean sorption energy, and ε is the Polanyi potential, which is equal to

$$\varepsilon = RT\ln(1 + 1/C_e) \quad (7)$$

where R is the gas constant (kJ/mol K) and T is the temperature (K). The saturation limit X_m represents the total specific micropore volume of the sorbent. The sorption potential is independent of the temperature but varies according to the nature of sorbent and sorbate (Khan et al., 1995). The slope of the plot of ln C_{ads} versus ε gives β (mol^2/J^2) and the intercept yields the sorption capacity, X_m (mol/g). The sorption space in the vicinity of a solid surface is characterized by a series of equipotential surfaces having the same sorption potential. This sorption potential is independent of the temperature but varies according to the nature of sorbent and sorbate. The sorption energy can also be worked out using the following relationship:

$$E = 1/\sqrt{-2\beta} \quad (8)$$

It is known that magnitude of apparent adsorption energy E is useful for estimating the type of adsorption and if this value is below 8 kJ/mol the adsorption type can be explained by physical adsorption, between 8 and 16 kJ/mol the adsorption type can be explained by ion exchange, and over 16 kJ/mol the adsorption type can be explained by a stronger chemical adsorption than ion exchange (Lin and Juang, 2002; Wang et al., 2004; Krishna et al., 2000).

The plot of ln C_{ads} against ε^2 for metal ion sorption on nano-HAp is shown in Fig. 5(c).

The Langmuir, Freundlich and D–R adsorption constants from the isotherms and their correlation coefficients are also presented in Table 2.

The correlation factors R (0.995, 0.934 and 0.942 for Langmuir, Freundlich and D–R model, respectively) confirm good agreement between both theoretical models and our experimental results. The maximum sorption capacity, Q_0, calculated from Langmuir equation is 46.17 mg/g, while Langmuir constant K is 0.07 L/mg. The values obtained for Ni^{2+} from the Freundlich model showed a maximum adsorption capacity (K_f) of 8.87 mg/g with an affinity value (n) equal to 2.74. The values of sorption constants, derived from D–R model are: 120.56 mg/g (2.05 mmol/g) for X_m, -4×10^{-9} mol^2/J^2 for β and 11.18 kJ/mol for E.

Table 2 Langmuir, Freundlich and D–R constants for adsorption of Ni^{2+} onto nano-hydroxyapatite.

Langmuir adsorption isotherms constants	
Q_0 (mg/g)	46.17
K (L/mg)	0.07
R^2	0.995
Freundlich adsorption isotherms constants	
k_f (mg/g)	8.87
n	2.74
R^2	0.934
D–R adsorption isotherms constants	
X_m (mg/g)	120.56
β (mol^2/J^3)	-4×10^{-9}
R^2	0.942

The values indicate that the adsorption pattern for Ni^{2+} on nano-HAp followed third the Langmuir isotherm ($R^2 > 0.995$), the D–R isotherm ($R^2 > 0.942$), and the Freundlich isotherm ($R^2 > 0.934$) at all experiments. It is clear that the Langmuir isotherm has best fitted for the sorption of Ni^{2+} on nano-HAp. When the system is in a state of equilibrium, the distribution of Ni^{2+} between the nano-HAp and the Ni^{2+} solution is of fundamental importance in determining the maximum sorption capacity of nano-HAp for the Ni^{2+} ion from the isotherm. The E values are 11.18 kJ for Ni^{2+}, on the nano-HAp. It is the orders of an ion-exchange mechanism, in which the sorption energy lies within 8–16 kJ/mol.

Generally, HAp selectivity towards divalent metal cations is a result of the ion-exchange process with Ca^{2+} ions (Monteil Rivera and Fedoroff, 2002). Ionic radius of Ni^{2+} (0.72 Å) slightly differ from that of Ca^{2+} (0.99 Å), and it can substitute Ca^{2+} in the HAp crystal lattice. Fig. 6 presents the XRD patterns of Ni^{2+}-loaded sample. No structural changes of nano-HAp were detected by the powder X-ray diffraction analysis of the solid residue with maximum amount of uptake capacity of Ni^{2+}, obtained after interaction 0.8 g/L of nano-HAp with 80 mg/L Ni^{2+} solution, at pH 6.6, at 300 rpm with 120 min of contact time. The sample was indexed in the hexagonal system with space group $P6_3/m$. The diffractograms evidences clarify that all XRD peaks were shifted toward upper diffraction angles for Ni-HAp particles (maximum peak: from $2\theta = 31.94°$ to $2\theta = 32.06°$). These shifts are indicative to the decrease in unit cell dimensions which is due to the replacement of Ni^{2+} (ionic radius 0.72 Å), which is smaller than Ca^{2+} (ionic radius 0.99 Å), into the crystal lattice of apatite molecules.

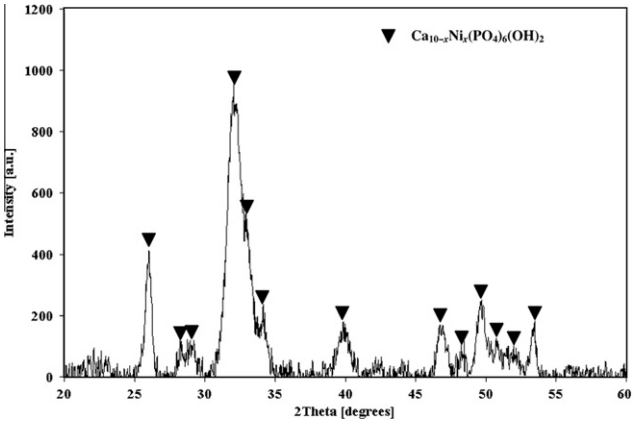

Figure 6 XRD pattern of the solid residue with maximum amount of uptake capacity of Ni^{2+} (pH 6.6, initial metal concentration = 80 mg/L, adsorbent dosage = 0.8 g/L, 300 rpm agitating rate).

The reaction mechanism corresponds to equimolar exchange of nickel and calcium yielding $Ca_{10-x}Ni_x(PO_4)_6(OH)_2$, where x can vary from 0 to 10 depending on the reaction time and experimental conditions. Our results of synthesized nano-HAp agreed with those described elsewhere that the proposed mechanism for Ni^{2+} removal by HAp comprises two steps: firstly, rapid surface complexation of the Ni^{2+} on the $\equiv$POH sites of the HAp which causes the decrease of the pH (from pH 6.6 to 6.2 for initial metal concentration = 80 mg/L, dosage = 0.8 g/L, 300 rpm agitating rate) and secondly, partial dissolution of calcium followed by the precipitation of an apatite with formula: $Ni_xCa_{10-x}(PO_4)_6(OH)_2$.

In which Ni^{2+} ions are first adsorbed on the nano-HAp surface and substitution with Ca^{2+} ion occurs as described by the following equation:

$$Ca_{10}(PO_4)_6(OH)_2 + xNi^{2+} \rightarrow Ca_{10-x}Ni_x(PO_4)_6(OH)_2 + xCa^{2+} \quad (9)$$

The values of the adsorption capacities for the adsorption of Ni^{2+} cations on different adsorbents used in the literature with adsorbent of the present study are summarized in Table 3. Although direct comparison of the nano-HAp with other adsorbent materials is difficult, owing to the differences in experimental conditions, it was found that the adsorption capacity of nano-HAp was higher than adsorbents presented in Table 3.

4. Conclusions

The present investigation shows that the nano-HAp is an effective adsorbent for the removal Ni^{2+} from aqueous Ni^{2+} solutions. The aqueous Ni concentration (80 mg/L) at 5 min was reduced to 51 mg/L by nano-HAp. The adsorption process is a function of the adsorbent dosage, the initial Ni^{2+} concentra-

Table 3 Adsorption capacities for sorption of Ni^{2+} by various adsorbents.

Adsorbents	Adsorption capacity (mg/g)	Reference
Chabazite	4.5	Ouki and Kavannagh (1999)
Clinoptilolite	0.9	Ouki and Kavannagh (1999)
Alternanthera philoxeroides biomass	9.73	Wang and Qin (2006)
Waste of tea factory	18.42	Padilha et al. (2005)
PAC	31.08	Rao et al. (2002)
Fly ash	0.03	Rao et al. (2002)
Bagasse	0.001	Rao et al. (2002)
Baker's yeast	11.40	Patmavathy et al. (2003)
Sheep manure waste	7.20	Abu Al-Rub et al. (2002)
Sphagnum moss peat	9.18	Ho et al. (1995)
Succinated alfalfa biomass	8.5	Gardea-Torresdey et al. (1998)
Calcium-alginate	10.5	Huang et al. (1996)
Cone biomass of *Thuja orientalis*	12.42	Malkoc (2006)
Nano-hydroxyapatite	46.17	Present work

tion and the temperature. The efficiency of Ni^{2+} adsorption increased with an increase in the adsorbent dosage. Isotherm studies indicate that the Langmuir model fits the experimental data better than Freundlich and D–R model. The adsorption equilibrium was described well by the Langmuir isotherm model with maximum adsorption capacity of 46.17 mg/g of Ni^{2+} ions on nano-HAp.

The results of XRD analysis strongly support the ion exchange as a main mechanism for Ni^{2+} removal by nano-HAp. The results show that the Ni^{2+} uptake by nano-hydroxyapatite proceeds with a rapid surface complexation of the Ni^{2+} on the $\equiv$POH site before the formation of a compound of formula $Ca_{10-x}Ni_x(PO_4)_6(OH)_2$. Thermodynamic calculations showed that the Ni^{2+} sorption process of nano-HAp has endothermic and spontaneous nature.

Acknowledgments

This research was supported by the Research Project Unit at the Materials and Energy Research Center, Karaj, Iran under the project No. 388873.

References

Abu Al-Rub, F., Kandah, M., Aldabaibeh, N., 2002. Nickel removal from aqueous solutions using sheep manure wastes. Eng. Life Sci. 2, 111–116.

Aksu, Z., 2002. Determination of the equilibrium, kinetic and thermodynamic parameters of the batch biosorption of nickel(II) ions onto *Chlorella vulgaris*. Process Biochem. 38, 89–99.

Aksu, Z., Tezer, S., 2005. Biosorption of reactive dyes on the green alga *Chlorella vulgaris*. Process Biochem. 40, 1347–1361.

Canet, L., Ilpide, M., Seta, P., 2002. Efficient facilitated transport of lead, cadmium, zinc and silver across a flat sheet-supported liquid membrane mediated by lasalocid A. Sep. Sci. Technol. 37, 1851–1860.

Chen, X., Wright, J.V., Conca, J.L., Peurrung, L.M., 1997. Effects of pH on heavy metal sorption on mineral apatite. Environ. Sci. Technol. 31, 624–631.

Czerniczyniec, M., Farias, S., Magallanes, J., Cicerone, D., 2003. Arsenic adsorption on biogenic HAP: solution composition effects. In: 11th International Conference on Surface and Colloid Science, Foz do Iguazu, Brazil, pp. 269.

Dŏgan, M., Alkan, M., 2003. Adsorption kinetics of methyl violet onto perlite. Chemosphere 50, 517–528.

Doan, H.D., Wu, J., Mitzakov, R., 2006. Combined electrochemical and biological treatment of industrial wastewater using porous electrodes. J. Chem. Technol. Biotechnol. 81, 1398–1408.

Elliott, J.C., 1994. Structure and Chemistry of the Apatites and Other Calcium Orthophosphates. Elsevier, Amsterdam.

Esalah, O.J., Weber, M.E., Vera, J.H., 2000. Removal of lead, cadmium and zinc from aqueous solutions by precipitation with sodium di-(n-octyl) phosphinate. Can. J. Chem. Eng. 78, 948–954.

Fuller, C., Bargar, J., Davis, J., Piana, M., 2002. Mechanisms of uranium interactions with hydroxyapatite: implications for groundwater remediation. Environ. Sci. Technol. 36, 158–165.

Gardea-Torresdey, J.L., Tiemann, K.J., Dokken, K.I.,Gamez, G., 1998. Investigation of metal binding in alfalfa biomass through chemical modification of amino and sulfhydryl ligands. In: Proceedings of the 1998 Conference on Hazardous Waste Research, pp. 111–121.

Hasany, S.M., Saeed, M.M., Ahmed, M., Radioanal, J., 2002. Sorption and thermodynamic behavior of zinc(II)–thiocyanate complexes onto polyurethane foam from acidic solutions. Nucl. Chem. 252, 477–484.

Ho, Y.S., 2003. Removal of copper ions from aqueous solution by tree fern. Water Res. 37, 2323–2330.

Ho, Y.S., JohnWase, D.A., Forster, C.F., 1995. Batch nickel removal from aqueous solution by Sphagnum moss peat. Water Res. 29, 1327–1332.

Huang, C., Ying-Chien, C., Ming-Ren, L., 1996. Adsorption of Cu(II) and Ni(II) by palletized biopolymer. J. Hazard. Mater. 45, 265–267.

Kadirvelu, K., Thamaraiselvi, K., Namasivayam, C., 2001. Adsorption of nickel(II) from aqueous solution onto activated carbon prepared from coirpith. Sep. Purif. Technol. 24, 497–505.

Khan, S.A., Rehman, U.R., Khan, M.A., 1995. Adsorption of chromium (III), chromium (VI) and silver (I) on bentonite. Waste Manage. 15, 271–282.

Krestou, A., Xenidis, A., Panias, D., 2004. Mechanism of aqueous uranium (VI) uptake by a natural zeolitic tuff. Miner. Eng. 16, 1363–1370.

Krishna, B.S., Murty, D.S.R., Prakash, B.S.J., 2000. Thermodynamics of chromium(VI) anionic species sorption onto surfactant-modified montmorillonite clay. J. Colloid Interface Sci. 229, 230–236.

Langmuir, I., 1918. The adsorption of gases on plane surfaces of glass, mica and platinum. J. Am. Chem. Soc. 40, 1361–1403.

Laperche, V., Traina, S.J., Gaddam, P., Logan, T.J., Ryan, J.A., 1996. Chemical and mineralogical characterizations of Pb in a contaminated soil: reactions with synthetic apatite. Environ. Sci. Technol. 30, 3321–3326.

Leyva, A., Marrero, J., Smichowski, P., Cicerone, D., 2001. Sorption of antimony onto hydroxyapatite. Environ. Sci. Technol. 35, 3669–3675.

Lin, S.H., Juang, R.S., 2002. Heavy metal removal from water by sorption using surfactant-modified montmorillonite. J. Hazard. Mater. B 92, 315–326.

Ma, Q.Y., Traina, S.J., Logan, T.J., Ryan, J.A., 1993. In situ lead immobilization by apatite. Environ. Sci. Technol. 27, 1803–1810.

Ma, Q.Y., Traina, S.J., Logan, T.J., Ryan, J.A., 1994. Effects of Aqueous Al, Cd, Cu, Fe(II), Ni, and Zn on Pb immobilization by hydroxyapatite. Environ. Sci. Technol. 28, 1219–1228.

Malkoc, E., 2006. Ni(II) removal from aqueous solutions using cone biomass of *Thuja orientalis*. J. Hazard. Mater. B137, 899–908.

Malkoc, E., Nuhŏglu, Y., 2003. The removal of chromium(VI) from synthetic wastewater by *Ulothrix zonata*. Fresenius Environ. Bull. 12, 376–381.

Mavropoulos, E., Rossi, A.M., Costa, A.M., Perez, C.A., Moreira, J.C., Saldanha, M., 2002. Studies on the mechanisms of lead immobilization by hydroxyapatite. Environ. Sci. Technol. 36, 1625–1629.

McGrellis, S., Serafini, J., Jean, J., Pastol, J., Fedoroff, M., 2001. Influence of the sorption protocol on the uptake of Cd ions in calcium hydroxyapatite. Sep. Purif. Technol. 24, 129–138.

Miretzky, P., Saralegui, A., Cirelli, A.F., 2006. Simultaneous heavy metal removal mechanism by dead macrophytes. Chemosphere 62, 247–254.

Mobasherpour, I., Soulati Heshajin, M., Kazemzadeh, A., Zakeri, M., 2007. Synthesis of nanocrystalline hydroxyapatite by using precipitation method. J. Alloys Compd. 430, 330–333.

Monteil Rivera, F., Fedoroff, M., 2002. Sorption of inorganic species on apatites from aqueous solutions. In: Encyclopedia of Surface and Colloid Science. Marcel Dekker, Inc., New York.

Nzihou, A., Sharrock, P., 2002. Calcium phosphate stabilization of fly ash with chloride extraction. Waste Manage. 2002, 235–239.

Ouki, S.K., Kavannagh, M., 1999. Treatment of metals-contaminated wastewaters by use of natural zeolites. Water Sci. Technol. 39, 115–122.

Padilha, F.P., Pessôa de Franc, F., Augusto da Costa, A.C., 2005. The use of waste biomass of *Sargassum* sp. for the adsorption of copper

from simulated semiconductor effluents. Bioresour. Technol. 96, 1511–1517.

Patmavathy, V., Vasudevan, P., Dhingra, S.C., 2003. Adsorption of nickel(II) ions on Baker's yeast. Process Biochem. 38, 1389–1395.

Rao, M., Parwate, A.V., Bhole, A.G., 2002. Removal of Cr6+ and Ni2+ from aqueous solution using bagasse and fly ash. Waste Manage. 22, 821–830.

Ravindran, V., Stevens, M.R., Badriyha, B.N., Pirbazari, M., 1999. Modeling the sorption of toxic metals on chelant-impregnated adsorbent. AIChE J. 45, 1135–1146.

Reichert, J., Binner, J., 1996. An evaluation of hydroxyapatite-based filters for removal of heavy metal ions from aqueous solutions. J. Mater. Sci. 31, 1231–1241.

Schiewer, S., Volesky, B., 1995. Modeling of the proton–metal ion exchange in biosorption. Environ. Sci. Technol. 29, 3029–3058.

Takeuchi, Y., Arai, H., 1990. Removal of coexisting Pb^{2+}, Cu^{2+}, Cd^{2+} ions from water by addition of hydroxyapatite powder. J. Chem. Eng. Jpn. 23, 75–80.

Tanaka, H., Futaoka, M., Hino, R., Kandori, K., Ishikawa, T., 2005. Structure of synthetic calcium hydroxyapatite particles modified with pyrophosphoric acid. J. Colloid Interface Sci. 283, 609–612.

Toles, C.A., Marshall, W.E., 2002. Copper ion removal by almond shell carbons and commercial carbons: batch and column studies. Sep. Sci. Technol. 37, 2369–2383.

Vega, E.D., Pedregosa, J.C., Narda, G.E., 1999. Interaction of oxovanadium(IV) with crystalline calcium hydroxyapatite: surface mechanism with no structural modification. J. Phys. Chem. Solids 60, 759–766.

Wang, C.C., Juang, L.C., Lee, C.K., Hsua, T.C., Leeb, J.F., Chaob, H.P., 2004. Effects of exchanged surfactant cations on the pore structure and adsorption characteristics of montmorillonite. J. Colloid Interface Sci. 280, 27–35.

Wang, X.S., Qin, Y., 2006. Removal of Ni(II), Zn(II) and Cr(VI) from aqueous solution by *Alternanthera philoxeroides* biomass. J. Hazard. Mater. B138, 582–588.

Zouboulis, A.I., Matis, K.A., Lanara, B.G., Loos-Neskovic, C., 1997. Removal of cadmium from dilute solutions by hydroxyapatite. II. Floatation studies. Sep. Sci. Technol. 32, 1755–1767.